IN FIELD MEASUREMENTS ON A SMALL SCALE OWC DEVICE

P. Filianoti[1] S. M. Camporeale[2]

[1] University Mediterranean of Reggio Calabria – Okeanòs Laboratory
e-mail: filianoti@unirc.it
[2] "Politecnico di Bari" University –DIMEG Department
E-mail: camporeale@poliba.it

Abstract

A 1:10 scale model of an ocean OWC breakwater was realised and put at the sea off the beach of Reggio Calabria (Italy). The breakwater (about 16 m long and 3.5 m height) was placed on a 2.1 m bottom depth, and embodied the REWEC wave energy converter (Boccotti *et al.*,2007, J. of Ocean Engineering, 34, 820-841). A small scale Wells turbine was installed onto the central caisson of the breakwater. Two different experiments were carried out. The first one aimed to test the energy absorption capabilities of the system and to analyse the waves-absorber interaction mechanism. The second experiment aimed to test the Wells turbine under oscillating randomly varying flows produced into the plant by sea waves. The goals of these experiments involved some measurements made critical because of the harsh environment, the high variability of randomly oscillating flows and unavoidable scale effects. Here, we show how these measurement difficulties were overcome by developing " ad hoc" measurements techniques. In particular, in this paper some critical measurements are described: the measurement of the water discharge through the plant, necessary to estimate the absorbed power; the instantaneous value of the torque exerted by the air flow on the turbine, necessary to analyse the actual unsteady behaviour of the turbine. Both measurements were carried out by using two different techniques, in order to make them robust.

Water discharge were calculated by integrating the acceleration of the water column, by recording the pressure simultaneously in different point along the streamline. This punctual measurement was compared with measurements carried out by an ultrasonic probe located on the roof of the plenum chamber. Because of the width of the sound beam, this measurement is space averaged.

Torque measurements were carried out by using the DC motor coupled with the Wells turbine as an electro-mechanical transducer. The procedure proved to be accurate once calibrated. A not trivial task was to separate, in the unsteady randomly varying reverse flow, the share of power transferred to the blade by the air current, from the shaft power driving the turbine, being necessary to sustain the rotation of the wheel many times in the cycle, because of high incidence of friction power losses in the small scale model.

Keywords: OWC, Wells turbine, unsteady performance, hysteresis.

Nomenclature

a	= acceleration
A	= section area
A_t	= turbine bladed area
b	= length of a single caisson
C_D	= discharge coefficient
H_s	= significant wave height
g	= acceleration of gravity
J	= momentum of inertia
K	= characteristic constant of the electric machine
n	= rotational speed
p	= pressure
p_a	= pressure in the air pocket
P_p	= pneumatic power supplied across the turbine
P_t	= blade turbine power
Q	= water flow in the caisson
R	= resonant coefficient
R_{tip}	= blade tip radius
s	= width of the vertical duct
s'	= width of the OWC
T	= torque
T_p	= peak period of the spectrum
V	= axial flow velocity
Δp_t	= pressure drop across the turbine
Δp_w	= wave pressure fluctuation at the outer opening of the plant
Greek	
ζ	= height of the air pocket
ζ_0	= still water value of ζ
ρ	= water density
ρ_a	= air density
Φ_{in}	= energy flux of the incident waves
Φ_p	= energy flux absorbed by the plant
ϕ	= flow coefficient

η = turbine efficiency
ω = turbine angular speed

Superscript

* = non-dimensional values
$^-$ = expected value

Subscript

a = air
A = OWC horizontal section at air-water interface
B = vertical duct horizontal section at the outer opening
el = electric
f = friction
J = power losses due to resistance (Joule) heating
p = plant, pneumatic, peak
t = turbine
0 = still value

1 Introduction

One of the most promising system for wave energy conversion is given by the Oscillating Water Column (OWC) devices (see, e.g., Falcão [1]) that are on-shore or near-shore systems that consist of a box with a big vertical opening in the front wall. Waves enter through this opening with only small diffraction effects from the front wall (see Sarmento and Falcão [2]), and propagate on the water surface in the box. On the roof of the box, there is a tube connecting the atmosphere with the air pocket between the water surface and the roof. This tube contains a Wells turbine (cfr. Raghunathan, [3]). The air pocket inside the box is compressed and expanded, alternately. As a consequence, an alternating air flow is produced that drives the turbine.

REWEC plants (Boccotti, [4],[5],[6], and [7]) are breakwaters in reinforced concrete embodying an OWC with a small opening. The experiment described here concerned the REWEC3 [7] that is a system in part beneath the sea level and in part above the sea level. The air pocket of the REWEC3 is connected with the atmosphere through a tube where a Wells turbine is installed. The size (width and length) of the vertical duct, and the sizes (length and height) of the room, and the diameter of the air tube are designed so that the eigenperiod is close to wave period.

The REWEC3 is valuable for two main reasons[8]:

(i) it has a structure very close to the well-established structure of conventional caisson breakwaters;

(ii) unlike conventional OWC devices, it exploits a natural resonance with sea waves, leading to very large absorption of wave energy; more than the 70% of the incident wave energy in a year is estimated to be absorbed.

Boccotti et al. [9] showed the results of a small scale field experiment on a breakwater (called REWEC). The plant is the 1:10 scale model (with some modifications) of a hypothesis of breakwater for the North-East Pacific coast. Figure 1 shows one of the nine caissons of the small-scale breakwater built in the natural laboratory of Reggio Calabria. Each caisson consists of three cells connected one to each other through holes H, so that air can flow from one cell to another of the same caisson.

Unlike the experiments described by Boccotti et al. in [9], in the experiment described here, a small Wells turbine was installed in the central caisson of the breakwater. Two views of the breakwater and of the duct hosting the installed turbine are given in Figure 1 and Figure 2 while a picture of the Wells turbine manufactured for this experiment is given in Figure 3.

The experiment, described in the present paper, had two main aims:

- to analyse the energy conversion from the fluctuating water flow at the outer opening of the vertical duct of the REWEC to the fluctuating air motion across the turbine;
- to evaluate the performance of the Wells turbine under real, randomly varying, sea conditions, that are most difficult to reproduce in laboratory.

Our plant at sea is able to produce high speed alternating currents with high frequencies spontaneously, and therefore it can be considered as a wind tunnel able to produce randomly alternated airflow having power spectra similar to those induced by sea waves. It is undoubtedly the ideal environment for testing Wells turbines.

2 Description of the experiment

2.1 Description of absorber breakwater

The breakwater built in the natural laboratory of Reggio Calabria was 16.3 m long, and it was realized by nine caissons close, one to each other. Each caisson consists of three interconnected cells, in that air can flow from one cell to another of the same caisson (the air flows through holes H in Figure 1). The central caisson is equipped with a small scale prototype_of Wells turbine.

2.2 Absorber performance parameter

The REWEC3 is able to work in resonance with waves. This matter depends essentially on the resonance coefficient

$$R = \frac{4T_{p-q}}{T_p}, \qquad (1)$$

where T_{p-q} is the lag of the absolute maximum of the cross-correlation between the wave pressure $\Delta p(t)$ on the outer opening of the vertical duct and the water discharge $Q_p(t)$ (positive if the water enters the plant) trough the plant. This coefficient, introduced in [10], ranges from -1 to 1. It is equal to zero if $\Delta p(t)$ is in phase with $Q_p(t)$, the plant works in a resonance condition R>0 means that the eigenperiod of the plant is greater than the wave period. R<0 means that the eigenperiod of the plant is smaller than the wave period.

3 Turbine and driving system

A small prototype of a monoplane Wells turbine without guide vanes has been built for the experiment.

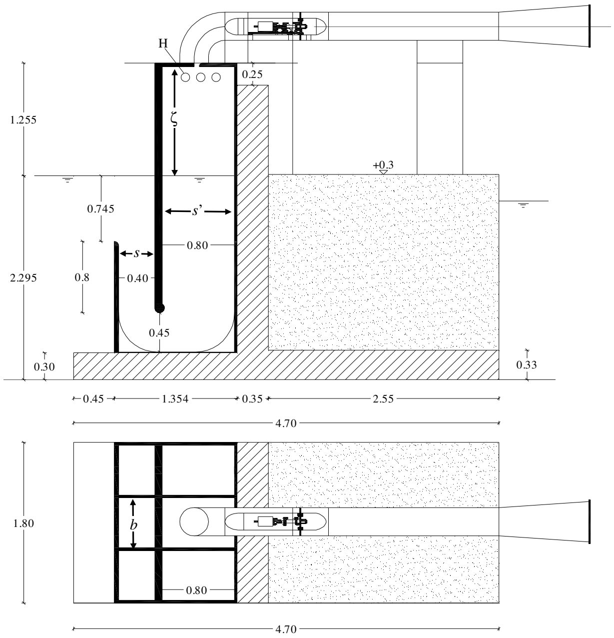

Figure 1 -The central caisson of the absorber breakwater where was installed the turbine. [measures are in meters and referred to the m.w.l.]

Figure 2 .- Pictures of breakwater and duct hosting the Wells turbine.

The Wells turbine prototype – see Figure 3 – designed to be coupled with this breakwater, is characterized by the following parameters: R_{hub} =101mm, R_{tip} =155mm, blade chord c=74mm, number of blades N =7, constant chord NACA0015 blade profile. Therefore, the hub-to-tip ratio and the solidity are equal to 0.65 and 0.64, respectively. The hub, divided into two parts, is made up of aluminium and comes from a commercial fan. The blades were manufactured in composite material reinforced by carbon fibre and were attached to the hub with a stagger angle of 90 deg.

Before the experiment was realised at sea, the turbine prototype was tested in an open wind tunnel facility, under steady state conditions, in order to determine the stationary characteristic curves. Details on this experiment are given in Torresi *et al.*[12].

The permanent magnet DC motor joined to the shaft of the turbine had a double function: it was operated as a power generator when pneumatic power of the air flow was high enough to allow the turbine to produce energy, and behaved as a motor when it was necessary to start the turbine (this is not to able to self start) and when it was necessary to support it because the pneumatic power was not sufficient to ensure the rotation speed set-up.

An electronic power device was purposely designed and realised in order to operate the turbine during the experiment. The device provided the following actions:

(i) to supply current to the electric motor at start-up, in order to accelerate the turbine up to the rotational speed sufficient to give a torque;

(ii) to act as a variable resistive load able to dissipate the electrical energy produced by the electrical motor when acting as a dynamo;

(iii) to switch from one to other of the above working conditions, in order to maintain stable the rotational speed, under the rapid fluctuations of the torque produced by the oscillating motion of the air.

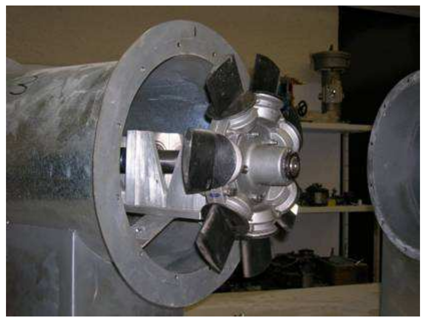

Figure 3.- The small scale model of the Wells turbine off the air tube.

All the actions (i)-(iii) were remotely controlled by a virtual instrument (VI) developed under LABVIEW® environment and running on a personal computer.

The variable resistive load was obtained by means of a bank of twelve resistors connected in parallel; each resistor was connected or disconnected to the bank through a mosfet acting as an electronic switch. The values of the conductance (the inverse of the resistance) of the twelve resistors were chosen to form a binary series; in this way the conductance of the overall bank can be varied from 1 up to 2^{12} times the minimum conductance in constant steps equal to the minimum conductance. By means of this arrangement it was possible to obtain a very rapid and practically "continuous" variation of the bank overall conductance.

The rotational speed was measured by means of a rotary encoder with a transmissive Optoschmitt Sensor. The rotational speed acquisition was made from the measurement of time period of the TTL signals generated by the encoder, in order to reduce the duty cycle of the software.

4 The experiment scenario

We measured

i) the energy flux of the incident waves;

ii) the energy flux absorbed by the plant;

iii) the energy flux of the pneumatic power delivered to the turbine

iv) the electric power generated by the turbine.

Details of the measurement techniques for measurements (i) and (ii) can be found in [9]. A summary of these techniques is given here.

Measurements (i) were obtained by means of a couple of ultrasonic probes placed in the undisturbed field, and for redundancy, by means of a couple of pressure transducers placed on the same vertical of the ultrasonic probes.

Measurements (ii) were obtained recording simultaneously, in each of three cells, the pressure fluctuations at the outer opening of the vertical duct and the surface displacement ζ of the water level inside the caisson. The level ζ in each cell was measured either directly by means of an ultrasonic probe or indirectly by means of three pressure transducers.

Measurements (iii) were obtained recording voltage and current at the electric terminals of the DC motor driving the turbine. Measurements of the turbine operating conditions are completed with the rotational speed. Measurements of power by means of current and voltage were considered more reliable than measurements of torque at the turbine shaft through a torquemeter, in consideration of the harsh environment where the turbine was operated and that, due to the low torque to be measured, shocks or handling might cause overload on the torquemeter. Moreover, recalibration of the load cell of the torquemeter, if necessary, would have been very difficult to realise after the turbine being installed on the breakwater. On the contrary, thanks to the very stable characteristics of the dc motor, it was possible to make reliable measurements of power through simultaneous measurements of current and voltage.

In all we had 22 signals (21 analogical and a TTL for the turbine tachometer) transmitted by submarine cables to a National Instrument (R)PXI data acquisition system, and recorded simultaneously at a rate of 10 samples / s per channel.

The turbine performance obtained from experiments is described by the following non-dimensional parameters.

- Torque coefficient T^*, defined as

$$T^* = \frac{T_t}{\rho_a \omega^2 R_{\text{tip}}^5} \quad (2)$$

where T_t is the torque referred to the internal (blade) power P_t

$$T_t = P_t / \omega , \quad (3)$$

ρ_a is the air density, ω is the angular speed, R_{tip} is the blade tip radius.

- The non-dimensional stagnation pressure drop Δp_0^*, defined as

$$\Delta p_0^* = \frac{\Delta p_0}{\rho_a \omega^2 R_{\text{tip}}^2} , \quad (4)$$

where Δp_0 is the stagnation pressure drop across the turbine.

- The flow coefficient, defined as

$$\phi = \frac{V}{\omega R_{\text{tip}}} , \quad (5)$$

where V is the average axial velocity in the turbine annulus, evaluated from the volumetric flow rate Q and the annulus area A_t from

$$V = \frac{Q}{A_t} . \quad (6)$$

5 Measurement technique

5.1 Measurement of the mean energy flux absorbed by the plant

The mean effective energy flux absorbed by a single cell was obtained from

$$\Phi_p = \left(\Delta p + \rho \frac{Q_p^2}{2b^2 s'^2} \right) Q_p , \quad (7)$$

where Δp is the pressure fluctuation at the mouth of the vertical duct and Q_p is the volumetric flow rate entering in the cell (assumed positive when entering the plant)

$$Q_p = -bs'' \frac{\mathrm{d}\zeta}{\mathrm{d}t} . \quad (8)$$

The mean energy flux absorbed by one cell may be re-written in the form [8]

$$\overline{\Phi}_p = \frac{1}{\mathsf{T}} bs'' \left[\Delta p(0)\zeta(0) - \Delta p(\mathsf{T})\zeta(\mathsf{T}) + \int_0^{\mathsf{T}} \zeta(t) \frac{\mathrm{d}\Delta p_w}{\mathrm{d}t} \mathrm{d}t \right] . \quad (9)$$

where Δp_w is the wave pressure fluctuation on the outer opening of the vertical duct, obtained by means of a pressure transducer at the centre of this opening.

For obtaining $\zeta(t)$ we used three pressure transducers. Two transducers A and B were placed inside the oscillating water column, the third one (transducer C) was in the air pocket. The actual height ζ of the water column proceeds from acceleration $a = (p_A - p_B - \rho g h)/(\rho h)$ calculated from the pressure difference between point A and point B and the pressure difference between point A (or B) and point C:

$$\zeta = \zeta_1 - \frac{p_A - p_C}{\rho(g+a)} \quad (10)$$

For checking the results, in cell 2 (the central one) we had a direct measurement made by a ultrasonic probe, and in cell 3 we had a fourth pressure transducer

(D) so that we obtained ζ by means of two triplet: A,B,C and B,D,C.

3.2 Measurement of the available pneumatic power

The pneumatic power P_p generated by the air flow rate Q is related to the pressure drop Δp_0 across the turbine

$$P_p = Q \Delta p_0 \,. \tag{11}$$

During the experiment on the REWEC system, the Wells turbine was operated under the action of the highly irregular air flow produced by the oscillating water level inside the chamber of the REWEC. Neglecting the effects of the compressibility of the air, the volumetric air flow rate Q crossing the turbine was assumed equal to the sum of the flow rates Q_p estimated from the fluctuations of the water level inside the three cells, as described in the previous sub-section. Since we had three interconnected chambers (only the central one being connected to the air duct of the turbine, see Figure 1) we evaluated the volumetric flow rate as

$$Q = \sum_{i=1}^{3} Q_i = \sum_{i=1}^{3} A_i \frac{d\zeta_i}{dt} \tag{12}$$

where A_i and ζ_i are the surface area and level of the water, respectively. Since the transfer of air from the lateral chambers to the central one is obtained through ports of known area and air pressure was recorded in all the chambers, it was possible to check the air flow rate Q_i (i=1, 3) from the lateral caissons to the central one from

$$Q_i = \pm C_D A_{p,i} \sqrt{2 \frac{|p_i - p_c|}{\rho_a}} \tag{13}$$

where $A_{p,i}$ is the geometric area of the port, C_D is the discharge coefficient, p_i-p_c is the pressure difference between the lateral caisson and the central one and, finally, ρ_a is the air density. Sign + in Eq.(13), is used if $p_i > p_c$ (air leaving the lateral caisson), while the sign – is used when $p_i < p_c$ (air entering the lateral caisson).

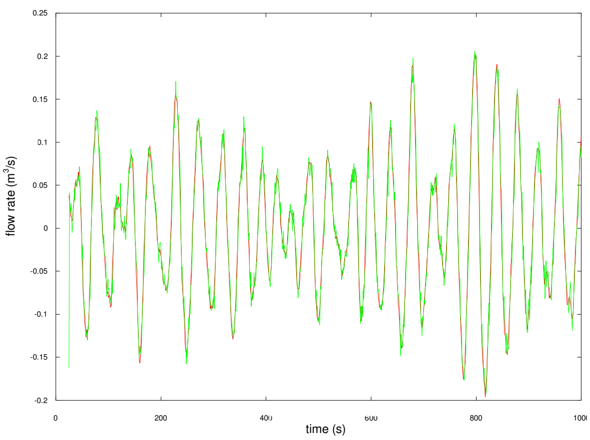

Figure 4 – Measurements of air flow rate from water level (red line) and pressure measurements (green line)

Figure 4 shows the time plots of the air flow rates obtained through the two methods: it appears a very good agreement between the two records, confirming the reliability of the method adopted for evaluating the air flow.

The pressure drop Δp_0 across the turbine was evaluated from the pressure difference between the pressure in the central cell and the atmospheric pressure, neglecting the pressure drops in the air duct due to minor losses at the air duct ends, in the curve and at the turbine hub. In order to reduce such losses the noses at the ends of the turbine-electric machine assembly, were streamlined. Actually, the geometry of the duct influenced the flow field across the turbine, as it was put in evidence by different results of the turbine performance when the flow was exiting from the chamber (outflow) and when the flow was entering the chamber (inflow). Such differences will be discussed later.

3.3 Unsteady measurements of the turbine performance

For the measurement of the turbine power output it was necessary to resort to a non-conventional methodology like the use of a torque-meter either of strain-gage or induction type would be. The very low torque developed by the turbine would have required a very sensitive instrument not suitable for the use in the field. A reliable and effective measurement procedure was specifically developed in order to evaluate the turbine power from measurements of current and voltage at the terminals of the brushed permanent magnet dc motor driving the turbine.

Preliminarily, measurements were carried out on the turbine-electric motor assembly under steady-state conditions realised in laboratory [12].

Being the electric machine a permanent magnet dc motor, the speed characteristic K_ω and the armature resistance R_a. were experimentally determined. The speed characteristic K_ω relates the electromotive force (e.m.f.) the angular velocity ω

$$\text{e.m.f.} = K_\omega \, \omega \,, \tag{14}$$

was determined during a deceleration test: the turbine was spun at a rotational speed of about 3000 rpm; then, the power source was disconnected and the turbine was left free of decelerate, without any connected load. The voltage at the terminals was measured and, as expected, a linear behaviour of the voltage as a function of the rotational speed was found (see Figure 5). Then, from a linear regression of the experimental points the value of the constant K_ω was obtained.

In a permanent magnet dc motor there is the particular property that the speed characteristic K_ω is equal to the torque characteristic K_T that relates the torque T_{el} of the electric machine to the current I

$$T_{el} = K_T I \,. \tag{15}$$

Since the dc motor is a reversible electric machine, the current I may be <0 or >0: in the first case, the dc machine acts as a motor and drives the turbine; in the second case, the turbine drives the dc motor that acts as a dynamo. Correspondingly, the turbine torque T_t is negative in the first case and positive in the second one.

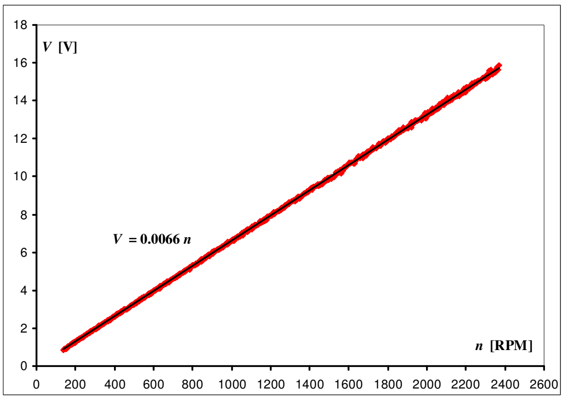

Figure 5 – Measurements of emf at the electric sockets of the dc motor during test without load.

In principle, by measuring the electric current, we would have got a very reliable method for measuring the torque exerted by the turbine. Unfortunately, the actual turbine torque T_t differs from the electric torque due to friction losses. Moreover, if the rotational speed undergoes fluctuations with time, the effects of the moment of the inertia of the turbine and of the other rotating parts (shaft and rotor of the electric machine).

Actually, notwithstanding the flywheel effect produced by the momentum of inertia of the turbine, the fluctuations of the pneumatic power cause significant oscillations of the rotational speed around the set point value. Therefore, taking into account the time derivative of the angular speed ω and the momentum of inertia J of all the connected rotating parts, the equation of the dynamic equilibrium of the rotating shaft can be written as

$$J\frac{\mathrm{d}\omega}{\mathrm{d}t} = T_t - T_{el} - T_f \tag{16}$$

where T_t is the torque exerted by fluid flow on the blade (we can call it as "blade torque") and T_f represent the torque exerted by the mechanical friction forces on the bearings and fluid-dynamic losses on the rotor.

Eq.(16) can be arranged in terms of unsteady power balance

$$J\omega\frac{\mathrm{d}\omega}{\mathrm{d}t} = P_t - P_{el} - P_J - P_f \tag{17}$$

where

- P_t is the fluid dynamic power exerted on the turbine blade by the fluid flow;
- $P_{el}=V\ I$ is the electric power measured at the electric motor;
- $P_J = R_a\ I^2$ is the electric power loss due to Joule effect;
- P_f is the overall friction power loss.

It should be noted that in Eq.(17) the term of the electric losses appears due to the fact that the voltage measured at the electric ends differs from e.m.f. of the voltage drop on the armature resistance. Since the armature resistance R_a is affected by variations due to usage and temperature, Eq.(16) gives more reliable measurements, even if both were used during the experiment giving about the same results.

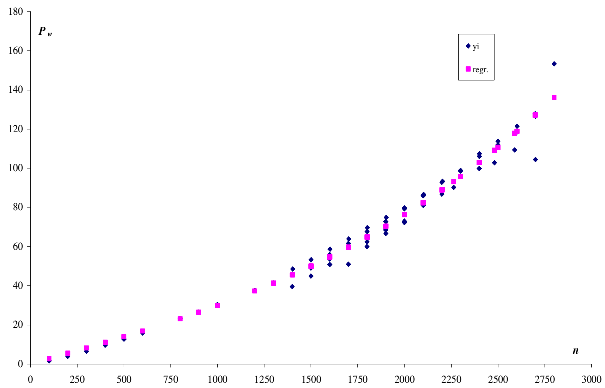

Figure 6 – Measurements of power losses under no air flow condition.

Tests at constant rotational speed, under no-flow conditions, were carried out to estimate friction losses. Figure 6 shows several measurements carried out at different rotational speed. A polynomial regression curve was obtained of the type

$$P_f = a\,n + b\,n^3, \tag{18}$$

where the linear term on the RHS of Eq.(18) is expected to reproduce friction power loss and the cubic term one is expected to take into account turbine winding power loss. A polynomial fit was adopted in order to estimate the constants a and b of Eq.(18).

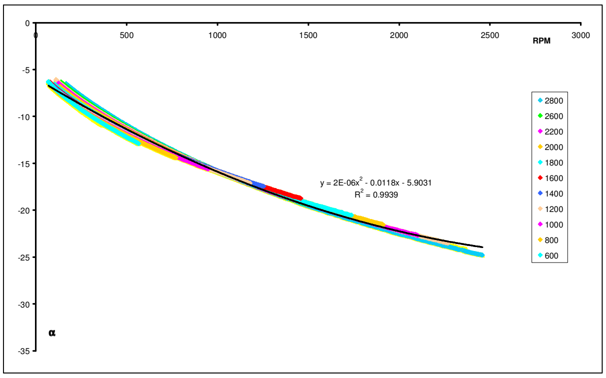

Figure 7 - Measurements of the derivative of the angular velocity during deceleration tests.

The results of the best fitting procedure showed that, up to a rotational speed of 2000 rpm, under no-flow conditions, about 87% of the total power losses are due to friction losses, while the remaining part is mainly due to heat losses in the internal electric resistance, while the losses due to winding effects are very small.

For measuring the unsteady torque exerted by the oscillating air flow on the turbine blade, it is necessary to evaluate the momentum of inertia J of the assembly composed by the rotating parts of the turbine and the electric machine. In order to determine the value of J the following testing procedure was developed: in laboratory, under no flow conditions, the turbine was spun up using the electric motor, then, the motor was switched off and the rotational speed was recorded with respect to time. Several tests of this kind were carried out starting from a different rotational speed. From such tests the derivative of the angular rotational speed $\alpha = \mathrm{d}\omega/\mathrm{d}t$ was evaluated as function of the rotational speed, as shown in Figure 7, where also a polynomial regression curve of all the experimental values is given.

From the measures of friction T_f and those of angular velocity derivative, $\mathrm{d}\omega/\mathrm{d}t$, it was possible to determine the momentum of inertia J. During the deceleration tests, since T_t and T_{el} are equal to zero, the dynamic equilibrium of the shaft gives

$$J\frac{\mathrm{d}\omega}{\mathrm{d}t} = -T_f \,. \tag{19}$$

Figure 8 shows the corresponding points of T_f and $\mathrm{d}\omega/\mathrm{d}t$ obtained during deceleration tests and the linear regression line that was used to calculate the momentum of inertia, J. A good coefficient of correlation was obtained that makes us confident in the obtained value.

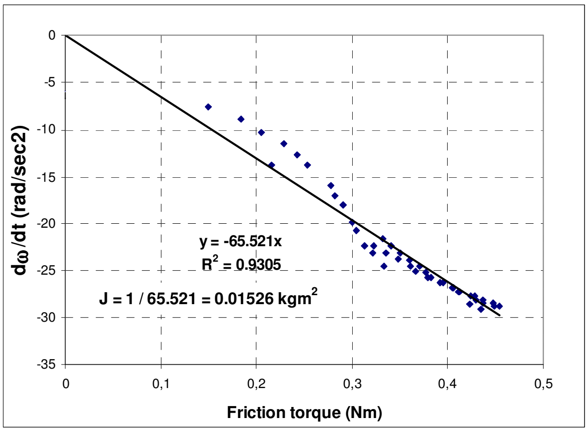

Figure 8 – Evaluation of the momentum of inertia from measurements of the derivative of the angular rotational speed.

Measurements of the turbine performance are extracted from measurement of voltage, current and rotational speed using the methodology developed for steady state measurements and described in Section 2.

In order to take into account the deterioration of the system due to the adverse turbine working conditions, the best fitting procedure adopted for evaluating friction losses has been periodically repeated under calm sea conditions.

6 In field measurements

The electric power driver was controlled via personal computer by means of a code written in LabVIEW environment. The control system is basically a PI (Proportional-Integral) closed loop controller able to fix the rotational speed to the set point. Under conditions when the turbine power output is negative, the DC motor is fed by a variable current in order to maintain the rotational speed around the set-point. Instead, when the time-average turbine power output is positive the DC motor, is connected to a bank of resistors that are able to behave as a variable resistance.

6.1 – Overall analysis of the unsteady performance of the turbine

We got 261 records; 73 records of wind waves, 61 records of wind waves superimposed on swells, a sequence of 95 records of swells of average T_p about 4 s, and a sequence of 32 records of swells of average T_p about 7.5 s.

An overview of the results is given in [14].

6.2 Pneumatic power

Figure 9 shows time records of pressure in the three connected chambers. It appears that the simultaneous values of pressure are about equal one to each other. A small pressure drop from the lateral chambers to the central one is observed when the pressure reaches the positive peaks while, vice versa, a drop from the central chamber to the lateral ones when the pressure reaches the negative peaks: such pressure drop is due to the pressure losses caused by the air flowing through the ports connecting the three chambers. The very small pressure drop between the connected chambers confirms that the assumptions that the compressibility effects are negligible is absolutely acceptable.

It is worth noting also that, otherwise what happens in the conventional OWC [1], there are not significantly differences in shape and amplitude of the fluctuations between the time in which the air is pumped out of the chamber and the time the air is aspired.

Figure 10 shows the time plots of the air flow for the three chambers during the same time interval considered in Figure 9. It appears that the simultaneous values of flow rate are about the same in the three cells.

The time plot of the pneumatic power produced in the time interval is given in Figure 11 . It appears that the frequency of the power oscillations is doubled with respect to the frequency of oscillation of pressure and flow and peaks of power reaches the value of hundreds of watts while the average power is much lower.

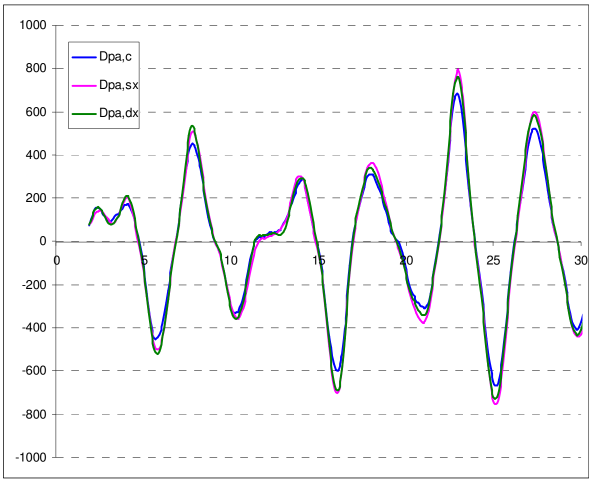

Figure 9 – Time plots of pressure inside the three chambers of the REWEC system. Pressure in mmH2O and time in seconds. (Dpa,c: central chamber; Dpa,sx: left side, Dpa,dx, right side)

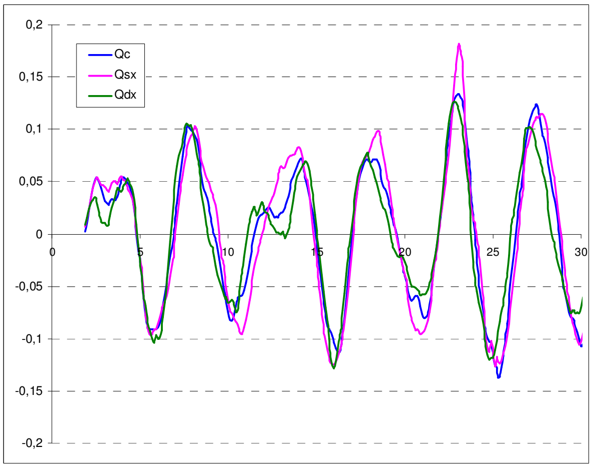

Figure 10 – Time plots of the air flow produced by the three chambers. Air flow in m^3/s and time in seconds. (Qc: central chamber; Qsx: left side, Qdx: right side)

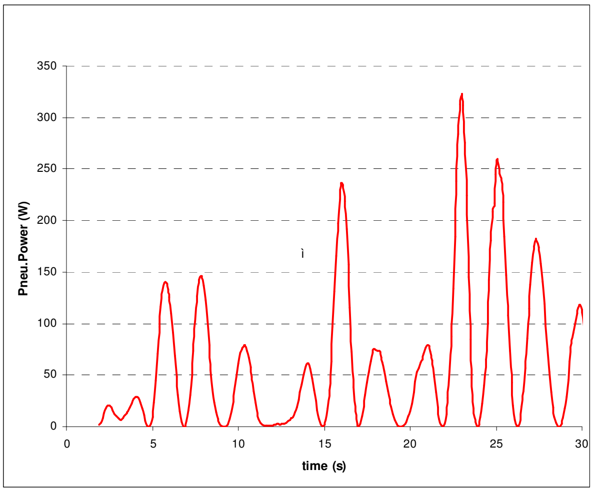

Figure 11 – Time plot of the pneumatic power.

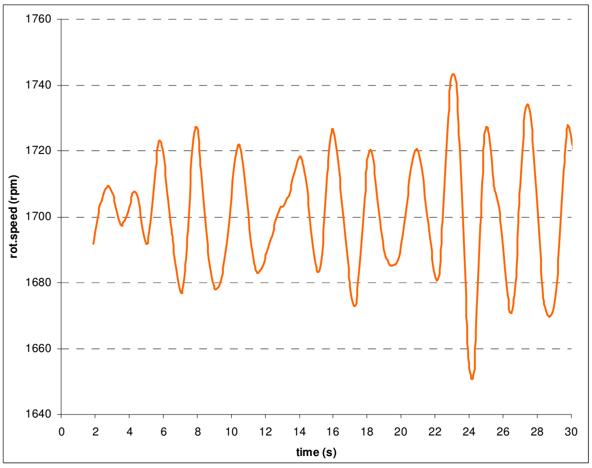

Figure 12 – A record of the oscillation of the rotational speed during the experiment.

6.3 Turbine unsteady performance

During the experiment the fluctuations of the pneumatic power cause a continuously varying torque, notwithstanding the flywheel effect of the turbine rotor. The effect of the variable torque was a variation of tens of rpm around the set-point, as shown in Figure 12. It appears that the control system was able to maintain the average turbine speed at the chosen value.

The blade turbine power was evaluated with two methodologies. With the first method (Met.(a) in Figure 13) we evaluated the turbine power from dynamic balance of power expressed by Eq.(17), by taking the measurements of the electric current, and taking into account friction losses, electric losses and fluctuations of the kinetic energy of the rotating assembly due to the derivative of the rotational speed.

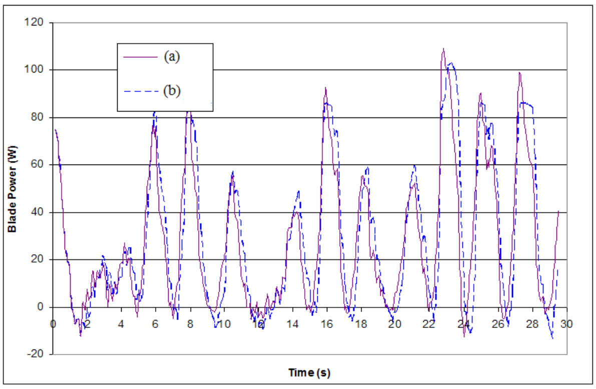

Figure 13 – Measurements of turbine power with two methodologies.

In the second method (Method (b) in Figure 13), we evaluated the blade turbine power neglecting the effects of the inertia of the rotating parts, after recognizing that, as far as concerns the dynamic behavior, the system can be described as a first order system that undergoes a fluctuating disturbance of about a constant frequency. The dynamic response of a first order system, if the frequency of the disturbance is lower than the cut-off frequency, is characterized by a magnitude that is about equal to value that would be obtained if the disturbance was applied “statically” (gain equal to 1) with a limited phase shift. In Figure 13 it appears that turbine output obtained with Method (b) is very close to that obtained with Method (a), with a time shift of about 0.3 seconds. The very good agreement between the measurements taken with the two methods, confirms that both the methodologies can be adopted if the frequency of the fluctuations of the pneumatic power is lower than the system’s cut-off frequency.From the measurement of pressure in the central chamber and the total flow rate evaluated using Eq.(12) the (instantaneous) non-dimensional pressure drop as a function of the flow rate has been obtained. It is worth noting that the pressure drop measured is such a way is a little different from the pressure drop across the turbine, since it includes pressure losses along the duct connecting the chamber to the atmosphere, at the air duct ends, and at the turbine hub. Anyhow, the presence of a separator in the curved connection of the chamber to the air duct, of the nose at both the inner duct ends, and metal sheets (supporting the turbine-electric motor assembly) that acts as guide vanes for the exiting flow, should have guided the flow patterns and contribute to reduce the pressure losses. However, the influence of the geometry of the air duct appeared to have a relevant influence on the power performance at the high flow rates, as it will be shown later. Finally, the effects of the unsteady flow of air column on the pressure on the pressure drop is limited, as shown in [12], and will be neglected here.

Figure 14 shows the results obtained for a record of 5 minutes at a sampling rate of 10samples/s. The positive values of ϕ represent the flow exiting the chamber towards the atmosphere. Negative values represent the entering flow condition: in such condition the pressure drop across the turbine is negative, meaning that the pressure inside the central chamber, which the turbine is connected to, is lower than the atmospheric pressure.

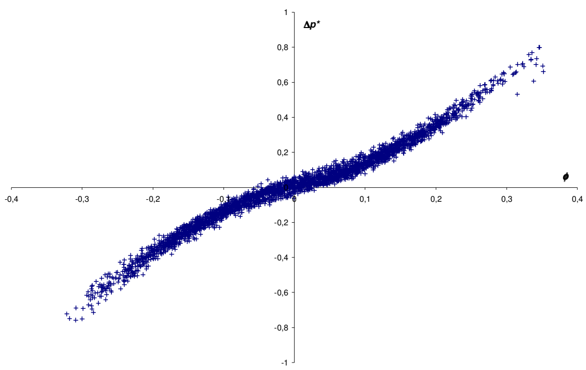

Figure 14 - Non-dimensional pressure drop vs flow coefficient

It appears that behaviour is close to be symmetric under inflow and outflow conditions, even if in outflow conditions, the maximum flow rate was about 0.35 higher than the absolute value of 0.32 obtained in the inflow condition. Moreover, the values of the pressure drops appear to be independent of the amplitude of the fluctuations.

From the measurements of the turbine (blade) power, the non-dimensional torque T^* is obtained as a function of the flow coefficient Figure 15. It appears that, in outflow condition, the maximum torque coefficient was higher than 0.12 while in inflow condition was always lower than 0.1. The turbine shows also negative torque coefficient with flow coefficient within the range $-0.1 < \phi < 0.1$. No stall conditions appear from these records.

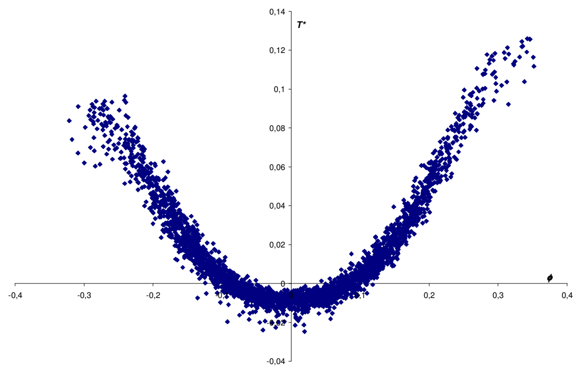

Figure 15 - Non-dimensional blade turbine torque vs. flow coefficient

The instantaneous values of turbine efficiency, evaluated from the data of pneumatic power and turbine power, are plotted in Figure 16. It appears that the maximum efficiency is about 0.45 that is a value relatively low in comparison with the results given by other authors, mainly due to the effects of the small dimensions of the turbine and, consequently, low Reynolds Number, as confirmed by steady state measurements and numerical results [12][13]. It is worth noting that the efficiency does not drop to zero, even with very high values of the flow coefficient. These aspects of the behaviour of the turbine will be discussed later.

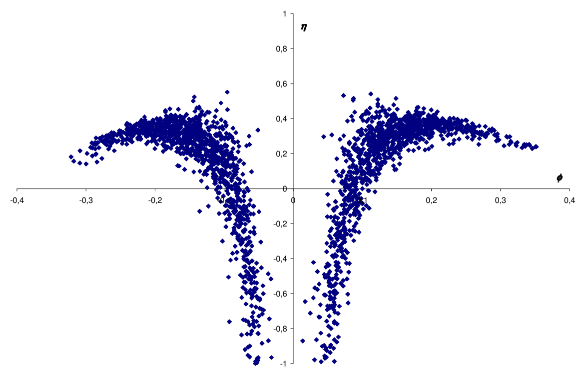

Figure 16 – Blade Turbine efficiency vs. flow coefficient

7 Regression analysis

As shown in preceding paragraph, the recorded values of torque coefficient show a certain dispersion, making it difficult to appreciate any signs of hysteresis between the acceleration and deceleration. For this purpose, the curves have been released subject to a process of regression of this kind: from the time history of the flow coefficient ϕ, the derivative $d\phi/dt$ was evaluated; then, the records with $d\phi/dt > 0$ were distinguished from those with $d\phi/dt < 0$. Then, the range of variation of the flow coefficient ϕ was divided in small intervals with amplitude equal to 0.01. From the records with flow coefficient falling in each interval, two mean values of the torque coefficient were evaluated as a function of ϕ: the first one was the mean value of T^* with $d\phi/dt > 0$, and the second one was the mean of those with $d\phi/dt > 0$.

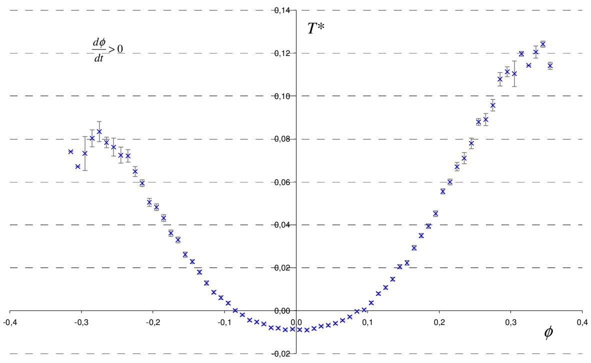

(a)

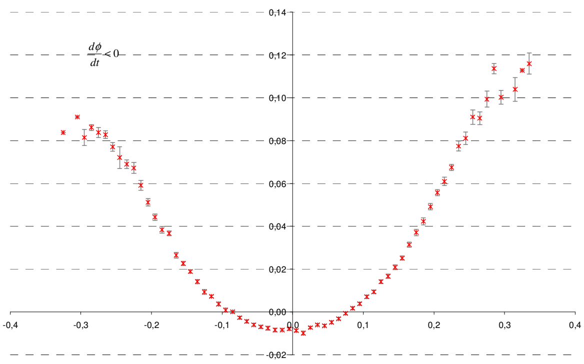

(b)

Figure 17 – Regression analysis for the torque coefficient.

Figure 17 (a) and (b) shows the results of such procedure: symbols represent the mean value while bars represent the standard deviation. It appears that the uncertainties are very small until $|\phi| < 0.2$. When absolute value of ϕ is higher, the uncertainties increase due to the lower number of available samples and the irregular behaviour of the turbine under incipient stall conditions. From the point of view of the measurement technique, the very small standard deviation that appears in a very large interval of variation of the flow coefficient confirms that the methodology adopted for compensating the effects on the torque measurements due to the fluctuations of the rotational speed is correct.

Figure 18 show comparison of the mean values of the torque coefficients: it appear that there are a few but appreciable differences between the results obtained with $d\phi/dt > 0$ and $d\phi/dt < 0$: this means that there is a little hysteretic behaviour of the turbine torque.

More significant differences are observed between the values of the torque coefficient obtained under outflow (ϕ>0) and under inflow (ϕ<0) conditions. It can be observed that the experimental values of T^* show a symmetric pattern with respect to y-axes until $|\phi|<0.22$. For higher values of $|\phi|$, the turbine performance show significant differences that, reasonably, are due to the influence of the geometry of the duct on the flow field and, consequently, on the behaviour of the turbine under incipient and deep stall conditions. A discussion on these topics and further results obtained during different records are given in a companion paper that is submitted to the conference [16].

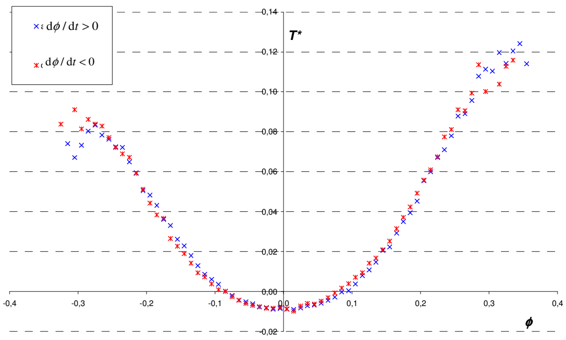

Figure 18 – Comparison of the mean torque coefficient obtained under increasing and decreasing flow coefficient

8 Conclusions

The paper describes the experiment on the REWEC3 system equipped with a monoplane Wells turbine without guide vanes and the measurement technique adopted to evaluate the wave energy conversion process and the unsteady behaviour of the turbine. In this paper it is shown that

(i) the measurements of flow rate based on the measurement of water level inside the chamber [10] give very good results as shown by the comparison of the flow rate through the connecting holes;

(ii) the characteristics of the permanent magnet dc electric machine driving the turbine have been obtained under laboratory tests; such characteristic enable us to use the electric machine as an electric transducer of the turbine torque;

(iii) the unsteadiness of the rotational speed influences significantly the measurements of torque: to overcome such problem the inertia of the rotating assembly was evaluated. The turbine blade power output was evaluated with two methods that give results in very good agreement.

(iv) the regression analysis show a very good repeatability of the measurements when the turbine is far from the incipient stall condition. Appreciable differences appear between the mean values recorded when the flow coefficient is increasing and those recorded with decreasing flow coefficient, giving the indication of a small hysteretic effect.
(v) there are significant differences in the turbine torque between inflow and outflow conditions, when the flow coefficient is relatively high. This appears to be reasonably due to the different flow field caused by the air duct geometry, that influences the turbine behaviour under incipient and deep stall conditions.

In conclusion, the described methodology appears to be reliable and suitable to give accurate results about the unsteady behaviour of the turbine, notwithstanding the difficulties related to take measurements under real sea wave conditions.

Acknowledgements

The experiment activities were partly supported by the Italian Research Ministry (MIUR) under the program "Relevant National Research Programs" (PRIN) within the project "New breakwaters for protecting coasts and converting wave energy into electric power".

The work of Dr. Mauro Giordani in designing, realising and maintaining the power device used for driving the electric machine during the experiment is gratefully acknowledged.

The careful work carried out by the graduated student Graziella Carlo during the analysis of the experimental data is very appreciated.

References

[1] Falcão A. F. de O., 2003 First-generation wave power plant: current status and R&D requirements, Proc. of OMAE2003; 22nd International Conference on Offshore Mechanics and Arctic Engineering, Cancun, Mexico.

[2] Sarmento A.J. and Falcão A.F. de O., 1985 Wave generation by an oscillating surface pressure and its application in wave-energy extraction.. J. Fluid Mech. 150, 467.

[3] Raghunathan S. 1995 The Wells air turbine for wave energy conversion. Prog. Aerospace Sci. 31, 335.

[4] Boccotti P., 2002. US Patent 6450732 B1.

[5] Boccotti P., 2003 On a new wave energy absorber. Ocean Eng. 30, 1191-1200.

[6] Boccotti P., 2003. European Patent EP 1133602 B1

[7] Boccotti P. 2007, European Patent EP 1518052 B1

[8] Boccotti P., 2007 Caisson breakwaters embodying an OWC with a small opening—Part I: Theory, Ocean Engineering 34, 806-819.

[9] Boccotti P., 2007 Comparison between a U-OWC and a conventional OWC", Ocean Engineering 34, 820-841.

[10] Boccotti P., Filianoti P., Fiamma V., Arena F. 2007, Caisson breakwaters embodying an OWC with a small opening—Part II: A small-scale field experiment, Ocean Engineering 34, 820-841.

[11] Camporeale S. M. and Filianoti P., 2007 A linearized model of OEC devices with additional vertical ducts, 7th European Wave and Tidal Energy Conference (EWTEC) , Porto, Portugal,.

[12] Torresi M., Camporeale S.M., and Pascazio G., 2007 Experimental and numerical investigation on the performance of a Wells turbine prototype, 7th European Wave and Tidal Energy Conference (EWTEC) , Porto, Portugal.

[13] Torresi M., Camporeale S. M.; Strippoli P. D., Pascazio G. 2008, "Accurate numerical simulation of a high solidity Wells turbine", Renewable Energy, 33 735–747

[14] Camporeale S.M., Filianoti P. (2008), "Energy Conversion of OWC Devices with Additional Vertical Ducts", Proceedings of the 27th International Conference on Offshore Mechanics and Arctic Engineering, OMAE 2008, Estoril, Portugal, 15-20 June 2008.

[15] Curran, R:, T. P. Stewart, T. J. T. Whittaker, 1997 Design synthesis of oscillating water column wave energy converters: performance matching, Proc. Inst. Mech. Eng., Part A - J. Power Energy 211, 489-505.

[16] Camporeale S.M., Filianoti P. (2009), Behaviour of a small Wells turbine under randomly varying oscillating flow, Proceedings of the 8th European Wave and Tidal Energy Conference, Uppsala, Sweden, 2009